Macromolecular Chemistry and Physics
www.mcp-journal.de

^{1}H PFG-NMR Diffusion Study on a Sequence-Defined Macromolecule: Confirming Monodispersity

*Xiaoai Guo, Katharina S. Wetzel, Susanne C. Solleder, Sebastian Spann, Michael A. R. Meier, Manfred Wilhelm, Burkhard Luy, and Gisela Guthausen**

A monodisperse decamer bearing ten different side chains, obtained via the iterative Passerini three-component reaction and subsequent deprotection, is investigated by ^{1}H pulsed field gradient (PFG) NMR. Both the stimulated echo (PFG-STE) and a fast spin-echo pulse sequence (β-PFG-SE) are applied to explore the translational diffusion properties of the sequence-defined decamer in solution at different concentrations with the aim of establishing an independent and new method to confirm its monodispersity. The signals decay according to the expectation of monodisperse molecules in solution with a high experimental accuracy, indeed verifying the monodispersity of these decamers. The diffusion coefficients can further be interpreted in terms of molecular weight. Both NMR methods result in comparable diffusion coefficients, while the β-PFG-SE reduces the experimental time by a factor of about 18.

1. Introduction

Sequence-defined macromolecules exhibit perfectly controlled primary structures and therefore are expected to become an important class of materials.[1–3] In contrast to sequence-controlled polymers, exhibiting a certain degree of dispersity ($Đ_M > 1$, typically 1.2 for controlled radical polymerization), sequence-defined polymers have a defined sequence of monomers and are uniform in size ($Đ_M \approx 1$).[2] As a new class of materials, synthetic sequence-defined macromolecules show unique structural properties and offer numerous application possibilities in the fields of data storage, catalysis, and artificial enzymes.[4–9] A recent review[10] summarizes various synthesis approaches toward sequence-defined macromolecules and discusses their individual advantages and disadvantages. Different synthesis approaches have been combined to achieve higher overall yields and to realize the desired oligomer structures.[11,12] Recently, the focus has been set on scalable and high-yield strategies for the synthesis of sequence-defined macromolecules.[13–16]

Polymer analytics play a key role in the polymer synthesis process, allowing for verification of the chemical structure and quality control. Characterization of sequence-defined macromolecules is especially challenging. The choice and definition of suitable and reliable methods depends on individual applications. Several analytical techniques are used for characterization of synthetic sequence-defined polymers,[2,17–20] for example, size exclusion chromatography (SEC), electrospray ionization mass spectrometry (ESI-MS), matrix-assisted laser desorption/ionization time-of-flight mass spectrometry (MALDI-ToF-MS), Fourier transform infrared (FT-IR) spectroscopy, and nuclear magnetic resonance (NMR). Recent studies showed that other promising tools, such as nanopore-based analytics[21,22] and electrospray ion beam deposition combined with high-resolution scanning tunneling microscopy (STM/ES-IBD)[23] are explored for sequence-defined polymer analysis.[2] It is noteworthy that some techniques are destructive for the analytes. For example, macromolecules are fragmented by collision-induced dissociation in tandem mass spectrometry (MS/MS), as the mass differences between the fragments are used to decode the monomer sequences.[2,24] SEC is often used to track the formation of building blocks and intermediates in synthesis, but requires calibration. The prepared sample is usually not recovered. A recent report from research groups of Meier and Barner-Kowollik[11] showed that the chromatographically determined dispersity is close to 1 ($Đ_M$ = 1.01–1.03) for the sequence-defined oligomers alternatingly consisting of Passerini and photoblocks, indicating

Dr. X. Guo, Prof. M. Wilhelm
Institute for Chemical Technology and Polymer Chemistry
Karlsruhe Institute of Technology (KIT)
Engesserstrasse 18, 76128 Karlsruhe, Germany
K. S. Wetzel, Dr. S. C. Solleder, Prof. M. A. R. Meier
Institute of Organic Chemistry (IOC)
Materialwissenschaftliches Zentrum (MZE)
Karlsruhe Institute of Technology (KIT)
Strasse am Forum 7, 76131 Karlsruhe, Germany
S. Spann, Prof. B. Luy
Institute of Organic Chemistry and Institute for Biological Interfaces 4
Karlsruhe Institute of Technology (KIT)
Fritz-Haber-Weg 6, 76131 Karlsruhe, Germany
Prof. G. Guthausen
Institute for Mechanical Process Engineering and Mechanics and Engler-Bunte-Institut
Chair of Water Chemistry and Water Technology
Karlsruhe Institute of Technology (KIT)
Adenauerring 20b, 76131 Karlsruhe, Germany
E-mail: gisela.guthausen@kit.edu

© 2019 The Authors. Published by WILEY-VCH Verlag GmbH & Co. KGaA, Weinheim. This is an open access article under the terms of the Creative Commons Attribution-NonCommercial License, which permits use, distribution and reproduction in any medium, provided the original work is properly cited and is not used for commercial purposes.

The copyright line for this article was changed on 20 October 2020 after original online publication.

DOI: 10.1002/macp.201900155

 © 2019 The Authors. Published by WILEY-VCH Verlag GmbH & Co. KGaA, Weinheim

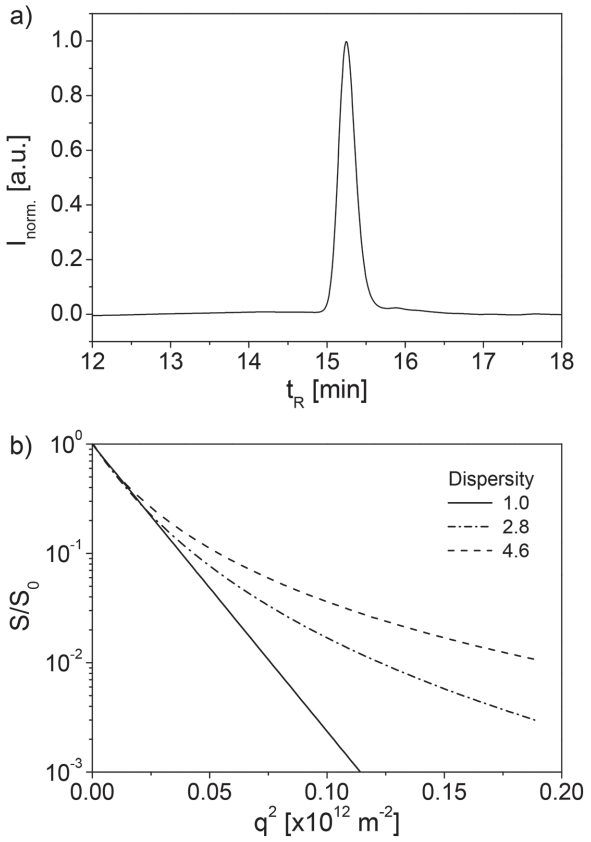

Figure 1. a) SEC of sequence-defined decamer. The concentration of the decamer was measured as a function of retention time t_R resulting in a peak with a finite width. b) Schematic diagram of raw signal decays (S/S_0) in PFG-NMR measurements for different and extreme dispersities $Đ_M$. The signal decay evidently deviates from the straight line for monodisperse molecules in solution ($Đ_M = 1$).

the monodisperse character of the macromolecules. However, peak broadening observed in SEC traces may be associated with the diffusion of the oligomers in the SEC column as shorter oligomers have larger mean square displacement due to thermal diffusion. Another possible reason may be the higher interaction of the—in contrast to the Passerini blocks—more polar photomonomers incorporated into the oligomer, resulting in an adsorption driven column interaction and thus a signal broadening. It should be mentioned that SEC measures weight fraction of a molecular weight as a function of retention time. In practice, $Đ_M = 1$ cannot be depicted precisely by SEC because even perfect monodisperse macromolecules cannot give a single elution time but rather show an elution time distribution with a certain width (**Figure 1**a). Nevertheless, SEC analysis is an important characterization technique for sequence-defined macromolecules, since it resolves even tiny amounts of impurities.

Compared to other analytical techniques, high-resolution NMR spectroscopy allows for direct observation of the chemical species with high spectral sensitivity and selectivity. A variety of NMR characterization techniques for polymeric systems are established.[25–28] More recently, an overview of the development of NMR spectroscopy with emphasis on applications in macromolecular science has been reported by Spiess.[17] So far, there have been few reports on pulsed field gradient NMR or diffusion-ordered spectroscopy (PFG-NMR/DOSY) study of synthetic sequence-defined oligomeric macromolecules.[29,30]

To overcome the challenge in characterization of sequence-defined macromolecules with dispersity close to 1, the diffusion properties of a sequence-defined decamer, which serves as a model oligomer system, were investigated by ^{1}H PFG-NMR. A major advantage of this NMR technique in comparison with other methods is that a nondestructive and noninvasive analysis can be performed while keeping the sample intact. Only small amounts of oligomers or polymers are needed. In addition, PFG-NMR was shown to allow for fast analysis of samples with different dispersity indices larger than one (Figure 1b). Signal decay curves in PFG-NMR were shown to deviate from that of monodisperse molecules in solution ($Đ_M = 1$), especially at larger q^2, which provides the basis for an intuitive and effective method to quantify the dispersity. However, it is worth mentioning that for polymers with high dispersity ($Đ_M \gg 1$), appropriate models such as the gamma distribution model should be used for the interpretation of NMR diffusion raw data.[31,32]

To achieve ten different and selectable side chains, a sequence-defined decamer was synthesized via iterative Passerini three-component reaction (P-3CR) and subsequent deprotection.[15] Both the stimulated echo (PFG-STE) and a fast spin-echo pulse sequence (β-PFG-SE) were applied to explore the diffusion properties of decamer solutions at different concentrations and confirm the monodispersity. The molecular weight determined by PFG-NMR is compared with those obtained with other methods, that is, theoretical expectations, ESI-MS, and SEC.

2. Experimental Section

2.1. Sequence-Defined Decamer

The studied decamer with ten different and selectable side chains, including aliphatic, aromatic, and olefinic side chains (**Figure 2**), was synthesized previously[15] and used herein as a model for the reported ^{1}H PFG-NMR studies.

The sequence-defined decamer was dissolved in 0.5 mL deuterated chloroform ($CDCl_3$, 99.8 atom% D, Euriso-Top) at different concentrations (0.2, 0.8, and 8 wt%). The decamer solutions were filled into 5 mm NMR tubes and sealed with parafilm to reduce solvent evaporation, that is, concentration changes. For the two PFG-NMR experiments carried out in this study, the samples were prepared individually.

2.2. SEC Measurements

SEC measurements were performed on a Shimadzu SEC system equipped with a Shimadzu isocratic pump (LC-20AD), a Shimadzu refractive index detector (24 °C) (RID-20A), a Shimadzu autosampler (SIL-20A), and a Varian column oven (510, 50 °C). For separation, a three-column setup was used with one SDV 3 µm, 8 × 50 mm precolumn and two SDV 3 µm, 1000 Å, 3 × 300 mm columns supplied by PSS, Germany.

© 2019 The Authors. Published by WILEY-VCH Verlag GmbH & Co. KGaA, Weinheim

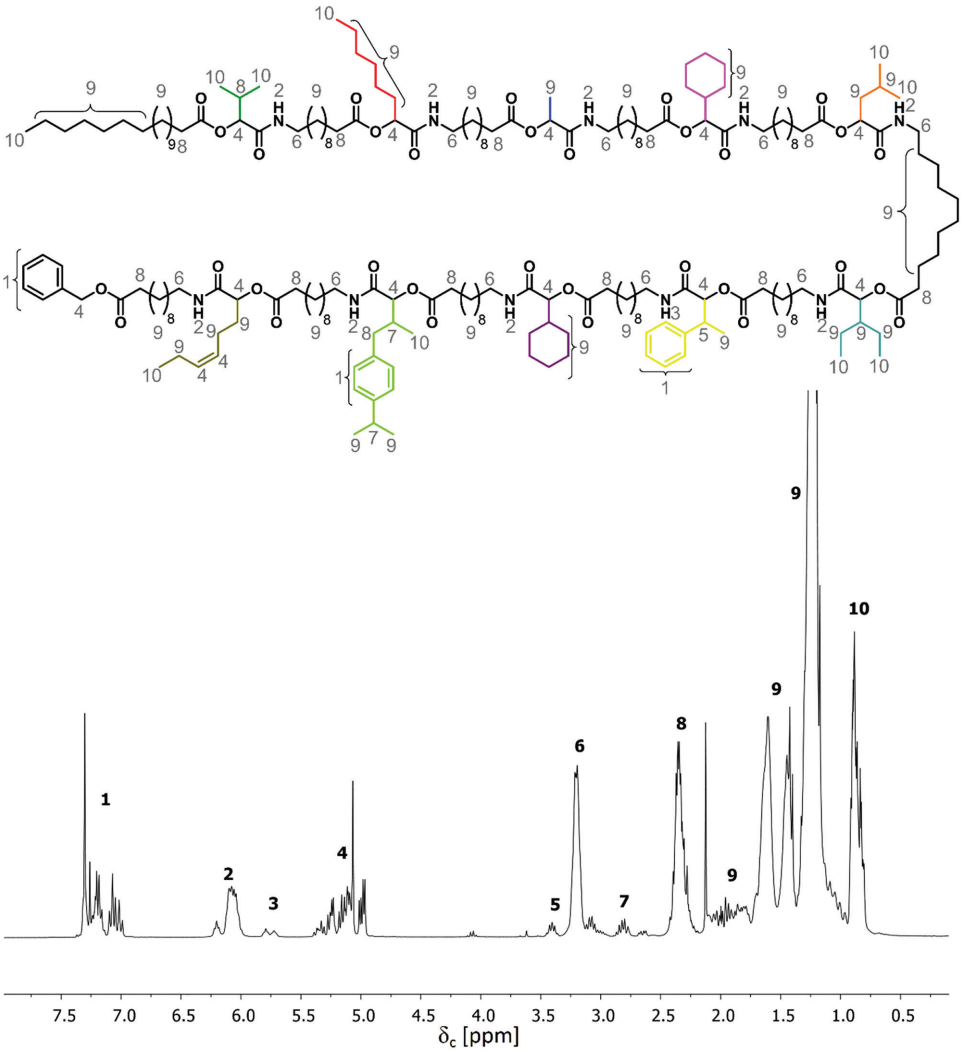

Figure 2. Structure of the investigated sequence-defined decamer bearing ten different side chains,[15] which was used in the ^{1}H PFG-NMR study. Numbers indicate the assignment of various chemical groups, which correspond to different chemical shifts δ_c in the ^{1}H NMR spectrum. NMR experiments were performed in deuterated chloroform.

Tetrahydrofuran stabilized with 250 ppm butylated hydroxytoluene (≥99.9%) supplied by Sigma-Aldrich was used at a flow rate of 1.0 mL min^{-1}. Calibration was carried out by injection of eight narrow polymethylmethacrylate (PMMA) standards ranging from 102 to 58 300 kDa.

2.3. PFG-NMR Diffusion Experiments

The ^{1}H PFG-NMR experiments were performed at room temperature 25 °C on a 400 MHz NMR spectrometer (Bruker Avance 400 WB, Bruker, Germany), that is, at 9.4 T. It was equipped with a diffusion probe DIFF BB, currently providing a maximum gradient strength g of up to 12 T m^{-1}. The spectra were acquired via PFG-STE with 32 linearly incremented gradient steps and 128 scans within Topspin 2.1 (Bruker, Germany) to provide an excellent signal-to-noise ratio. Parameters of ^{1}H PFG-NMR diffusion experiments are detailed in **Table 1**. In addition, inspired by the concept of Ernst angle,[33] a modified PFG-SE pulse sequence (β-PFG-SE, **Figure 3**) using a small excitation flip angle $\beta \leq 30°$ was applied for fast measurements on the decamer instead of the conventional 90° excitation pulse in a spin-echo sequence. The advantage is that the repetition time can be reduced drastically by a factor of more than 10 at a moderate reduction of signal intensity. To verify this approach, hexadecane was diluted with $CDCl_3$ (T_1 = 1.9 s). Both sequences were applied to compare the diffusion-attenuated signals (**Figure 4**) for confirmation of the principle of this fast version of PFG-NMR. The data could be modeled within the Stejskal–Tanner model[34] and revealed the following diffusion coefficients: $D_{\beta\text{-PFG-SE}} = 8.41 \times 10^{-10}$ m^2 s^{-1}, while $D_{\text{PFG-STE}} = 8.19 \times 10^{-10}$ m^2 s^{-1}. The deviation is in the order of 3%. The measurement time amounts to 2 min 15 s for the β-PFG-SE compared to 21 min 12 s needed for PFG-STE, which is due to full longitudinal relaxation in the latter case. The limitation of the β-PFG-SE is the T_2 limit for the diffusion time, which is essential when measuring large molecules, highly concentrated solutions with small (apparent)

© 2019 The Authors. Published by WILEY-VCH Verlag GmbH & Co. KGaA, Weinheim

Table 1. Parameters of ^{1}H PFG-NMR diffusion experiments.

Parameter	PFG-STE	β-PFG-SE
Gradient pulse duration, δ [ms]	2	2
Maximum gradient amplitude, g_{max} [T m^{-1}]	3	3
Gradient pulse stabilization time [ms]	1	1
Number of gradient steps	32	32
Diffusion time, Δ [ms]	40	40
Delay between the first 2 RF pulses, τ [ms]	4.16	–
Repetition time, T_R [s]	11	0.59
Number of scans	128	128
Number of dummy scans	2	4
Excitation pulse,[a)] P_1 [µs]	8.3 (90°)	3 (β = 23°)
180° pulse, P_2 [µs]	–	24
Spoiler gradient duration [ms]	2	–
Spoiler gradient amplitude [T m^{-1}]	0.083	–

[a)]High and low power level settings for the RF amplifier were used in the PFG-STE and β-PFG-SE experiments, respectively.

diffusion coefficients, or systems with geometric hindrance like emulsions.

The longitudinal relaxation of the decamer amounted to 1 s, but was chemical shift dependent. Therefore, a repetition time of 11 s was used for full magnetization build-up for PFG-STE, while the β-PFG-SE was performed at a repetition time of 0.59 s, which reduced the measurement time by a factor of 18. This factor, of course, depends on the longitudinal relaxation times of the species to be observed and on the expected experimental accuracy. Other experimental parameters are summarized in Table 1. The phase corrected data were integrated in the significant regions of the spectra. Further data processing was performed within home-written Matlab scripts.

3. Results and Discussion

The 1D ^{1}H-NMR spectrum of the decamer (Figure 2) shows the characteristic peaks, here labeled with numbers, as reported

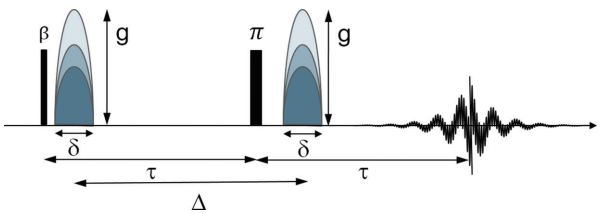

Figure 3. Fast pulsed field gradient spin-echo pulse sequence (β-PFG-SE). The black rectangles represent radio-frequency (RF) pulses. A β-pulse with a small excitation flip angle was used instead of the usually applied $\pi/2$-pulse according to the Ernst-angle principle. Spin refocusing is done via a π-pulse. The grey pulses between two RF pulses and after the π-pulse represent magnetic field gradient pulses with duration δ and gradient amplitude g. The time between two gradient pulses is the diffusion time Δ. The echo signal is acquired as a function of g, denoted by the free induction decay (FID) at 2τ after the β-pulse.

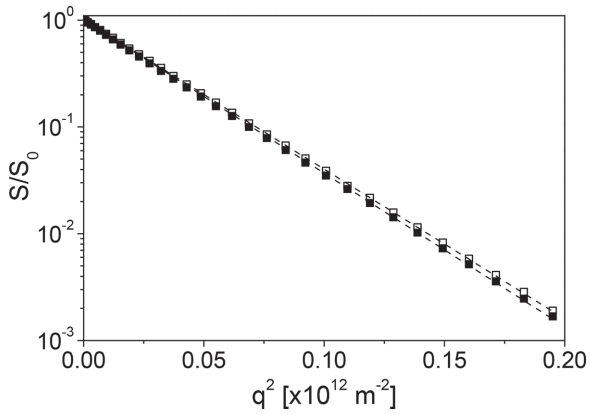

Figure 4. Comparison of the diffusion-attenuated signals for *n*-hexadecane diluted by $CDCl_3$ and measured with PFG-STE (□) and β-PFG-SE (■). The signal attenuation was modeled by the Stejskal–Tanner model for monodisperse molecules in solution (dashed line).

previously.[15] The lines in the spectrum correspond to various chemical groups of the studied decamer. In the ^{1}H PFG-STE NMR spectra, the signal intensity S depends on the amplitude of the magnetic field gradient g (**Figure 5**a), which is due to translational mobility of the decamer and allows to determine the diffusion coefficient. The same spectra were observed using the β-PFG-SE pulse sequence. All peaks visible in the acquired ^{1}H PFG-NMR spectra were analyzed. As a molecule diffuses as a whole, the normalized intensities of the diverse chemical groups coincide and reflect the accuracy of the diffusion measurements above the noise level (here $S/S_0 < 10^{-3}$, Figure 5b). This observation indicates that there are no major differences between the side chains and backbone groups (Figure 2) as expected, revealing a uniform diffusion of the oligomer in solution.

In the case of monodisperse molecules ($Đ_M = 1$) and without interference with other molecules, that is, at infinite dilution, the signal decay is described by a mono-exponential function in q^2 or a Gaussian function in q (dashed line in Figure 5c):[34]

$$\frac{S(q)}{S_0} = \exp[-Dq^2(\Delta - \delta/3)] \quad (1)$$

where S_0 is the signal intensity at $q = 0$, D the diffusion coefficient, and Δ the diffusion time. The parameter q is defined as the product $\gamma g \delta$, where γ is the ^{1}H gyromagnetic ratio, g the gradient amplitude, and δ the gradient pulse duration.

In the case of higher concentrations and/or molecular weight distributions, the mean free path length of diffusion is distributed and the NMR signal can be described by a gamma distribution (solid line in Figure 5c), which was shown for mass-distributed polymers.[31,32] Both models describe the experimental data well above the experimental noise level, while the width of the gamma distribution amounts to 1.3×10^{-11} m^2 s^{-1}, which is a rather low value in comparison to the mean diffusion coefficient 1.06×10^{-10} m^2 s^{-1}.

As it is well known that the concentration influences the translational diffusion of macromolecules, the decamer solution was characterized at three different concentrations (**Figure 6**a,b). It is obvious that the experimental data can be

© 2019 The Authors. Published by WILEY-VCH Verlag GmbH & Co. KGaA, Weinheim

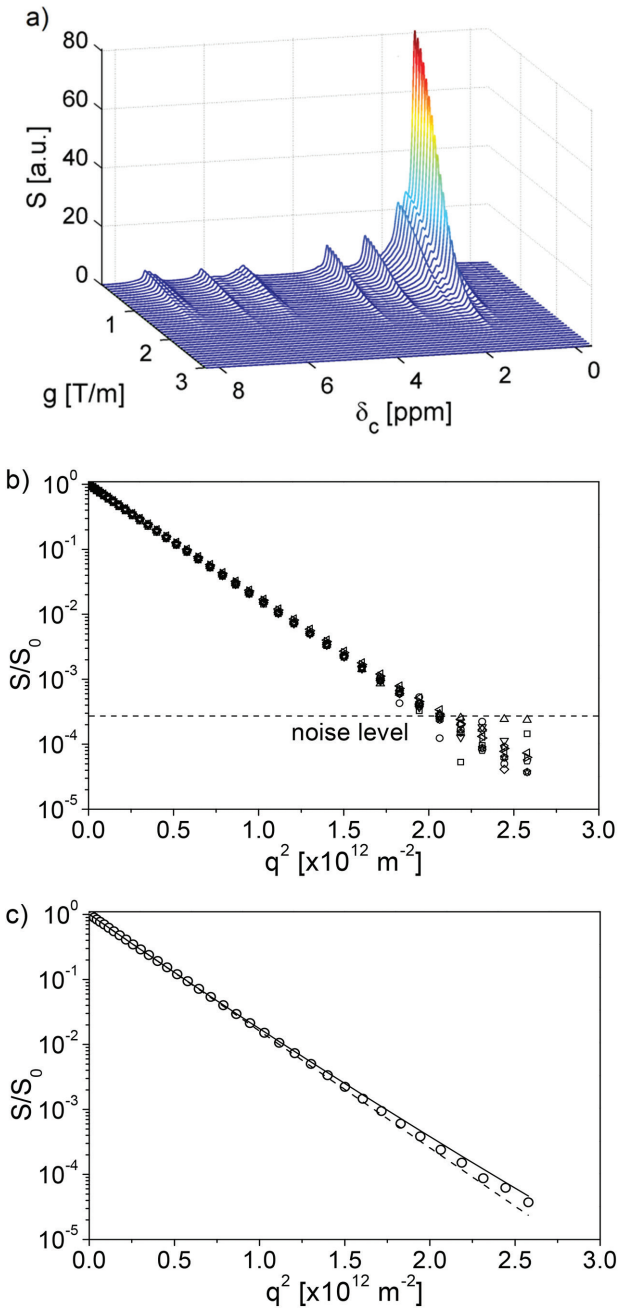

Figure 5. PFG-NMR on a decamer solution at a concentration of 8 wt%. a) ^{1}H PFG-STE NMR spectrum. b) Normalized signal decays S/S_0 for different peaks in the ^{1}H PFG-STE NMR spectrum. The dashed line indicates the noise level. c) Signal decay (○) of the peak at 1.27 ppm modeled within the Stejskal–Tanner model (dashed line) and a gamma distribution (solid line), respectively. Due to the relatively high concentration, a small deviation from the theoretical expectation is observed at large q^2, that is, low signal intensities. The relative standard deviation of the diffusion coefficients determined from the signal decays with different noises at large q^2 is at 1%.

very well described within the Stejskal–Tanner model at all three concentrations down to about the noise level (here $S/S_0 = 10^{-3}$), although the absolute NMR signals of course become noisier at lower concentrations. Corresponding diffusion coefficients (Figure 6d) decrease with increasing decamer concentration as expected.[32,35,36] There is only a small variation in the diffusion coefficients at concentrations of 0.2 and 0.8 wt%, for example, $D = (2.15 \pm 0.05) \times 10^{-10}$ m^2 s^{-1} for 0.2 wt% and $D = (1.99 \pm 0.03) \times 10^{-10}$ m^2 s^{-1} for 0.8 wt% in PFG-STE experiments (open symbols in Figure 6d). Further increasing decamer concentration leads to a decrease of the diffusion coefficient. Similar diffusion properties have been observed in the β-PFG-SE experiments, except that the slopes of signal decay curves are slightly steeper (Figure 6a–c) and thus leading to slightly larger diffusion coefficients (filled symbols in Figure 6d and **Table 2**). Apart from possible concentration differences due to individual sample preparation for the two experiments, intrinsic differences in the NMR pulse sequences (also see Figure 4) are to be mentioned; the fast repetition in the β-PFG-SE introduces a strong T_1 weighting, whereas the full magnetization is explored in the PFG-STE experiment. The relative deviation between diffusion coefficients obtained by PFG-STE and β-PFG-SE is about 9%, which is within a reasonable range. The concentration dependence of the diffusion coefficient can be described with the above-mentioned model (dashed lines in Figure 6d). The diffusion coefficient at 0.2 wt% is very close to that at the lower concentration limit.

In diverse studies, the diffusion coefficient D was linked to the molecular weight M_w by the following equation:[32,37,38]

$$D = K \cdot M_w^{-\alpha} \tag{2}$$

where K and α are scaling parameters relevant to the material under study.

In general, this power law holds true for sufficiently low concentrations. The question arose whether K and α are unique given that the diffusion was measured at lowest concentrations. To extend previous work, some dilute polymer solutions in $CDCl_3$[30,32,39,40] are summarized and the diffusion coefficients of the decamer in solution are added (**Figure 7**). Data are distributed around a trend line with $\alpha = 0.51$. The parameter α ranges between 0.4 and 0.6 in literature.[38] Both K and α depend on the studied molecular architecture and solvents. Crutchfield et al. reported the empirical power–law relation with molecular masses in the range of 2–1280 g mol^{-1} for dilute $CDCl_3$ solutions with a value of $\alpha = 0.58$.[41] Augé et al. obtained $\alpha \in [0.47, 0.61]$ for PS and PMMA in $CDCl_3$.[38] Chamignon et al.[40] studied the solution properties of poly(*N*-acryloylmorpholine) (PNAM) in various solvents while $\alpha \in [0.4, 0.47]$.

Compared to other linear polymers, for example, polystyrene, the diffusion coefficients of the dilute decamer solutions are smaller (Figure 7), implying a smaller α value, but still within the tolerated experimental uncertainty. To obtain the molecular weight of the decamer from these measurements, the diffusion coefficients of decamer molecules under study and some data points of polymer molecules with side chains from the literature, such as regioregular conjugated polymers (poly(3-hexylthiophene), P3HT_10, P3HT_20, P3HT_40),[30] were used to build a power-law relationship of $D = 6.87 \times 10^{-9} M_w^{-0.42}$. With that, the molecular weight of the decamer is determined to be 3664.1 g mol^{-1} by PFG-STE. This value is very close to the molecular weight of 3562.7 g mol^{-1}

© 2019 The Authors. Published by WILEY-VCH Verlag GmbH & Co. KGaA, Weinheim

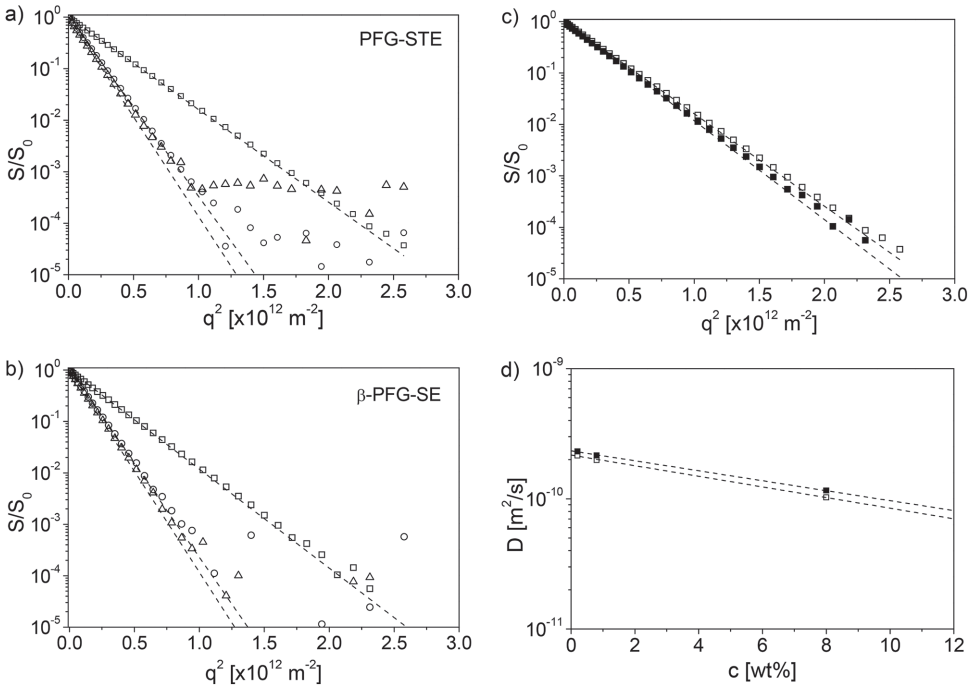

Figure 6. PFG-NMR results of decamer macromolecules at different concentrations. a) Signal decays acquired with PFG-STE (□: 8 wt%; ○: 0.8 wt%; Δ: 0.2 wt%; dashed lines: Stejskal–Tanner model). b) Signal decays acquired with β-PFG-SE (□: 8 wt%; ○: 0.8 wt%; Δ: 0.2 wt%; dashed lines: Stejskal–Tanner model). c) Comparison between signal decay curves acquired with both PFG-STE (□) and β-PFG-SE (■) at $c = 8$ wt% and modeled with the Stejskal–Tanner model (dashed line). d) Concentration dependence of the diffusion coefficients measured by PFG-STE (□) and β-PFG-SE (■). Dashed lines indicate mono-exponential fits.

theoretically calculated from the chemical composition $C_{212}H_{364}N_{10}O_{32}$ of the sequence-defined decamer. Additionally, the molecular weight by PFG-STE is in good agreement with the masses obtained by ESI-MS.[15] The observed doubly charged ions ($[M+2Na]^{2+}$ = 1804.4 m/z) of the sequence-defined decamer correspond to a molecular weight of 3562.7 g mol^{-1}. A similar molecular weight (3613.4 g mol^{-1}) was obtained from the diffusion coefficient measured by β-PFG-SE (Table 2). An overestimation of the molecular weight (4998.9 g/mol) results if the scaling relationship of $D = 1.8 \times 10^{-8} M_w^{-0.51}$ (trend line in Figure 7) was used. This can be attributed to different hydrodynamic characteristics of the decamer molecules under study and other polymers with different molecular architectures in solutions.

Table 2. Results of ^{1}H PFG-NMR diffusion experiments of decamer solutions at different concentrations.

Parameter	PFG-STE	β-PFG-SE	Chemical composition[a)]	ESI-MS[b)]
Diffusion coefficient D [$\times 10^{-10}$ m^2 s^{-1}]				
$c = 8.0$ wt%	1.03 ± 0.01	1.16 ± 0.05		
$c = 0.8$ wt%	1.99 ± 0.03	2.15 ± 0.13		
$c = 0.2$ wt%	2.15 ± 0.05	2.32 ± 0.15		
Noise level in signal decay, S/S_0	10^{-3}	10^{-3}		
Experiment time incl. acquisition time [s]	424	24		
Molecular weight M_w [g mol^{-1}]	3664.1	3613.4	3562.7	3562.7

[a)]Molecular weight calculated theoretically from the chemical composition ($C_{212}H_{364}N_{10}O_{32}$)[15]; [b)]Molecular weight determined by electrospray ionization mass spectrometry (ESI-MS)[15]; The errors are estimated from the differences in D of the diverse peaks in the spectrum.

The molecular weight obtained by SEC (6216 g mol^{-1}) was overestimated due to the peak broadening and calibration. It is found that in SEC measurement of such perfectly defined, monodisperse molecules ($Đ_M$ = 1), also verified in PFG-NMR experiments, the retention time did not give a single value but a peak with a finite width (Figure 1a). As discussed by Van Deemter et al.,[42] such a broadening results from several influencing factors. For instance, eddy diffusion effect arises from inhomogeneous packing and particle sizes in the SEC column, resulting in a variation of the analyte's flow paths through the column and thus a finite peak width instead of a single value near zero. Another effect is longitudinal diffusion or stronger diffusion of analyte molecules along the flow axis inside the column. Another explanation for the overestimation of molecular weight is the calibration via PMMA standards, whose characteristics differ significantly from the ones of the sequence-defined decamer in the SEC experiment, thus leading to inaccurate results in molecular weight. For determining the molecular weight distribution, on the other hand, SEC experiments provide more precise results. This study clearly demonstrates that both non-invasive PFG-NMR methods (PFG-STE

© 2019 The Authors. Published by WILEY-VCH Verlag GmbH & Co. KGaA, Weinheim

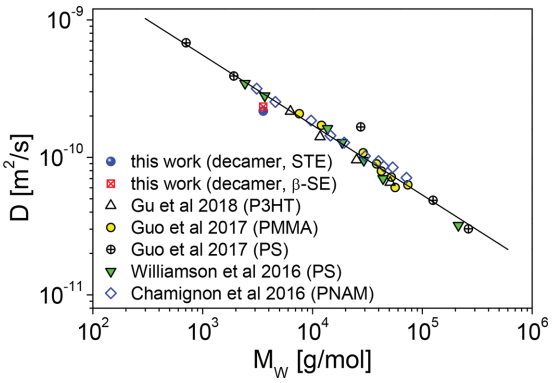

Figure 7. Correlation of diffusion coefficient D and molecular weight M_w in Equation (2) for dilute decamer solutions in $CDCl_3$ ($c = 0.2$ wt%) and dilute polymer solutions described in literature.[30,32,39,40] The solid line represents a trend line with $\alpha = 0.51$.

and β-PFG-SE) are well suitable for quantitative characterization of sequence-defined oligomers as well as other synthetic polymers, not only for determining the molecular weight distribution, but also for precisely estimating the molecular weight of monodisperse samples.

4. Conclusions

A sequence-defined decamer with ten different side chains was used as a model oligomer system, which was obtained via iterative Passerini P-3CR and subsequent deprotection as reported previously. Diffusion properties of these sequence-defined decamers in deuterated chloroform were studied at different concentrations of 0.2–8 wt% using ^{1}H pulsed field gradient stimulated echo (PFG-STE) and fast pulsed field gradient spin-echo (β-PFG-SE) NMR sequences. Both NMR methods give comparable results, but β-PFG-SE reduced the experimental measurement time by a factor of about 18. The acquired signal decays can be well described within the Stejskal–Tanner model with a high accuracy (down to the noise level of $S/S_0 = 10^{-3}$). This evidences the monodispersity of the synthesized decamer macromolecules and provides an alternative, convenient, and independent way of further confirming monodispersity in highly defined macromolecules with a high experimental accuracy while maintaining the oligomer. Moreover, the diffusion coefficient decreases with increasing decamer concentration due to the known concentration dependent molecular interactions. The relative deviation between diffusion coefficients obtained by PFG-STE and β-PFG-SE is about 9%, which is within a reasonable range. Finally, the molecular weight of the sequence-defined decamer was determined from ^{1}H PFG-NMR diffusion experiments and agrees well with expectations from the chemical structure and the value obtained by electrospray ionization mass spectrometry.[15] It should be pointed out that the diffusion properties of macromolecules depend on the molecular architecture and the solvent type. PFG-NMR can serve as a reliable, non-invasive, and non-destructive analytical alternative for quantitative characterization of sequence-defined oligomers as well as other synthetic polymers.

Acknowledgements

X.G. and K.S.W. contributed equally to this work. The authors gratefully acknowledge the financial support from the German Research Foundation (DFG SFB 1176 Project Q2, A3, and A1 as well as Pro²NMR instrumental facility at KIT).

Open access funding enabled and organized by Projekt DEAL.

Conflict of Interest

The authors declare no conflict of interest.

Keywords

diffusion, Passerini reaction, pulsed field gradient NMR, sequence-defined polymers

Received: April 12, 2019
Revised: August 1, 2019
Published online: August 29, 2019

[1] J.-F. Lutz, in *Sequence-Controlled Polymers: Synthesis, Self-Assembly, and Properties* (Eds: J.-F. Lutz, T. Y. Meyer, M. Ouchi, M. Sawamoto), American Chemical Society, Washington DC **2014**, p. 1.
[2] J.-F. Lutz, *Macromol. Rapid Commun.* **2017**, *38*, 1700582.
[3] J. De Neve, J. J. Haven, L. Maes, T. Junkers, *Polym. Chem.* **2018**, *9*, 4692.
[4] M. A. R. Meier, C. Barner-Kowollik, *Adv. Mater.* **2019**, *31*, 1806027.
[5] J.-F. Lutz, M. Ouchi, D. R. Liu, M. Sawamoto, *Science* **2013**, *341*, 1238149.
[6] A. C. Boukis, K. Reiter, M. Frölich, D. Hofheinz, M. A. R. Meier, *Nat. Commun.* **2018**, *9*, 1439.
[7] A. C. Boukis, M. A. R. Meier, *Eur. Polym. J.* **2018**, *104*, 32.
[8] S. Martens, A. Landuyt, P. Espeel, B. Devreese, P. Dawyndt, F. Du Prez, *Nat. Commun.* **2018**, *9*, 4451.
[9] T. Terashima, T. Mes, T. F. A. De Greef, M. A. J. Gillissen, P. Besenius, A. R. A. Palmans, E. W. Meijer, *J. Am. Chem. Soc.* **2011**, *133*, 4742.
[10] S. C. Solleder, R. V. Schneider, K. S. Wetzel, A. C. Boukis, M. A. R. Meier, *Macromol. Rapid Commun.* **2017**, *38*, 1600711.
[11] W. Konrad, F. R. Bloesser, K. S. Wetzel, A. C. Boukis, M. A. R. Meier, C. Barner-Kowollik, *Chem. - Eur. J.* **2018**, *24*, 3413.
[12] S. C. Solleder, S. Martens, P. Espeel, F. Du Prez, M. A. R. Meier, *Chem. - Eur. J.* **2017**, *23*, 13906.
[13] F. A. Leibfarth, J. A. Johnson, T. F. Jamison, *Proc. Natl. Acad. Sci. USA* **2015**, *112*, 10617.
[14] A. C. Wicker, F. A. Leibfarth, T. F. Jamison, *Polym. Chem.* **2017**, *8*, 5786.
[15] S. C. Solleder, D. Zengel, K. S. Wetzel, M. A. R. Meier, *Angew. Chem., Int. Ed.* **2016**, *55*, 1204.
[16] J. K. Szymański, Y. M. Abul-Haija, L. Cronin, *Acc. Chem. Res.* **2018**, *51*, 649.
[17] H. W. Spiess, *Macromolecules* **2017**, *50*, 1761.
[18] N. Zydziak, W. Konrad, F. Feist, S. Afonin, S. Weidner, C. Barner-Kowollik, *Nat. Commun.* **2016**, *7*, 13672.
[19] C. G. Smith, R. A. Nyquist, N. H. Mahle, P. B. Smith, S. J. Martin, A. J. Pasztor, *Anal. Chem.* **1987**, *59*, 119.
[20] J. H. Scrivens, A. T. Jackson, *Int. J. Mass Spectrom.* **2000**, *200*, 261.
[21] D. Branton, D. W. Deamer, A. Marziali, H. Bayley, S. A. Benner, T. Butler, M. Di Ventra, S. Garaj, A. Hibbs, X. Huang, S. B. Jovanovich, P. S. Krstic, S. Lindsay, X. S. Ling, C. H. Mastrangelo, A. Meller, J. S. Oliver, Y. V. Pershin, J. M. Ramsey, R. Riehn, G. V. Soni,

© 2019 The Authors. Published by WILEY-VCH Verlag GmbH & Co. KGaA, Weinheim

V. Tabard-Cossa, M. Wanunu, M. Wiggin, J. A. Schloss, *Nat. Biotechnol.* **2008**, *26*, 1146.
[22] Y.-L. Ying, J. Zhang, R. Gao, Y.-T. Long, *Angew. Chem., Int. Ed.* **2013**, *52*, 13154.
[23] S. Abb, L. Harnau, R. Gutzler, S. Rauschenbach, K. Kern, *Nat. Commun.* **2016**, *7*, 10335.
[24] L. Charles, C. Laure, J.-F. Lutz, R. K. Roy, *Rapid Commun. Mass Spectrom.* **2016**, *30*, 22.
[25] F. A. Bovey, P. A. Mirau, *NMR of Polymers*, Academic Press, San Diego **1996**.
[26] P. A. Mirau, in *Applied Polymer Science: 21st Century* (Eds: C. D. Craver, C. E. Carraher), Elsevier, New York **2000**, p. 787.
[27] H. N. Cheng, A. D. English, *NMR Spectroscopy of Polymers in Solution and in the Solid State*, American Chemical Society, Washington DC **2002**, p. 470.
[28] A. E. Tonelli, J. L. White, in *Physical Properties of Polymers Handbook* (Ed: J. E. Mark), Springer, New York **2007**, p. 359.
[29] J. S. Brown, Y. M. Acevedo, G. D. He, J. H. Freed, P. Clancy, C. A. Alabi, *Macromolecules* **2017**, *50*, 8731.
[30] K. Gu, J. Onorato, S. S. Xiao, C. K. Luscombe, Y.-L. Loo, *Chem. Mater.* **2018**, *30*, 570.
[31] M. Röding, D. Bernin, J. Jonasson, A. Särkkä, D. Topgaard, M. Rudemo, M. Nydén, *J. Magn. Reson.* **2012**, *222*, 105.
[32] X. Guo, E. Laryea, M. Wilhelm, B. Luy, H. Nirschl, G. Guthausen, *Macromol. Chem. Phys.* **2017**, *218*, 1600440.
[33] R. R. Ernst, W. A. Anderson, *Rev. Sci. Instrum.* **1966**, *37*, 93.
[34] E. O. Stejskal, J. E. Tanner, *J. Chem. Phys.* **1965**, *42*, 288.
[35] P. Gao, P. E. Fagerness, *Pharm. Res.* **1995**, *12*, 955.
[36] M. Cudaj, J. Cudaj, T. Hofe, B. Luy, M. Wilhelm, G. Guthausen, *Macromol. Chem. Phys.* **2012**, *213*, 1833.
[37] P. G. Gennes, *Scaling Concepts in Polymer Physics*, Cornell Universty Press, Ithaca **1979**.
[38] S. Augé, P.-O. Schmit, C. A. Crutchfield, M. T. Islam, D. J. Harris, E. Durand, M. Clemancey, A.-A. Quoineaud, J.-M. Lancelin, Y. Prigent, F. Taulelle, M.-A. Delsuc, *J. Phys. Chem. B* **2009**, *113*, 1914.
[39] N. H. Williamson, M. Nydén, M. Röding, *J. Magn. Reson.* **2016**, *267*, 54.
[40] C. Chamignon, D. Duret, M. T. Charreyre, A. Favier, *Macromol. Chem. Phys.* **2016**, *217*, 2286.
[41] C. A. Crutchfield, D. J. Harris, *J. Magn. Reson.* **2007**, *185*, 179.
[42] J. J. van Deemter, F. J. Zuiderweg, A. Klinkenberg, *Chem. Eng. Sci.* **1956**, *5*, 271.

© 2019 The Authors. Published by WILEY-VCH Verlag GmbH & Co. KGaA, Weinheim